International Journal of Heat and Technology
Vol. 42, No. 4, August, 2024, pp. 1385-1396
Journal homepage: http://iieta.org/journals/ijht

Thermal and Mechanical Analysis of Single U Welding Joint and Unsymmetrical Double U Welding Joint of Thick Steel Alloy Plates

Ola Hussein Ali Al-Tamermi[1*], Nabeh Alderoubi[2], Hasan Shakir Majdi[3], Haitham Mohammed Ibrahim Al-Zuhairi[4], Abdulghafor Mohammed Hashim[5], Laith Jaafer Habeeb[4]

[1] Training and Workshop Center, University of Wasit, Wasit 52001, Iraq
[2] Design and Drafting Technology Department, Lincoln Campus, Southeast Community College, Nebraska Lincoln 68521, USA
[3] Department of Chemical Engineering and Petroleum Industries, Al-Mustaqbal University College, Hillah 51001, Iraq
[4] Training and Workshop Center, University of Technology-Iraq, Baghdad 10066, Iraq
[5] Engineering of Technical Mechanical Power Department, Al-Amarah University College, Maysan 62001, Iraq

Corresponding Author Email: Olaa.H.Ali@uowasit.edu.iq

https://doi.org/10.18280/ijht.420428

Received: 31 May 2024
Revised: 3 August 2024
Accepted: 14 August 2024
Available online: 31 August 2024

Keywords:
unsymmetrical double U joints, fusion zone, normal stress, ANSYS simulation, deformation

ABSTRACT

The development of an accurate and meticulously designed simulation model for heat distribution during welding has helped maintain the popularity of welding as a reliable approach for attaching components. A simulated heat source involves uneven heating, resulting in uneven deformation and stress. An ANSYS simulation is used to analyze the stress in a welded flat plate. The simulation models are created using SOLIDWORKS software. The model employs the temperature-dependent characteristics of alloy steel to function as a thermal model that evaluates stress and the distribution of heat within the structure. This study offers a comprehensive examination of welded joints through the utilization of THERMO-MECHANICAL Finite Element Analysis (FEA) tools, specifically ANSYS. The study focuses especially on the analysis of single U and unsymmetrical double U welding connections. The study examined the heat distribution, thermal loads, and impacts on fixtures associated with welding, specifically focusing on the design of the welding joint. The results indicate that the heat from welding caused a maximum deformation of 0.55 mm for the single U joint and 0.54 mm for the double U welding joints. Both joint configurations displayed significant thermal stress at a distance of 5 mm from the center of the weld. According to the ANSYS models, the heat-affected zone (HAZ) has a length of 45.4 mm for a single U joint and 53.6 mm for an unsymmetrical double U joint. The second aspect of this investigation involves assessing the comparative durability or thermal strains of various depositions in the previously mentioned joint. Moreover, it is essential to assess the expected heat distortion and stress when examining prospective welding materials for on-site use. This will enhance the implementation of the material.

1. INTRODUCTION

Welding is a method of joining that is extensively utilized in the industry because of the generally recognized benefits, such as the reduction of costs and weight, the higher performance of structures that have been welded, and the flexibility available in the design process. Several different welding procedures have been developed over time [1]. Many other industry sectors continue to find the ongoing advancement of these procedures to be vital. Recent developments have generally concentrated on improving welding techniques, demonstrating their compatibility with cutting-edge materials, broadening the range of applications for these techniques, and gaining a better understanding of and overcoming the inherent limitations of the process. Regarding the latter, welding technologists must resolve the considerable temperature variations formed during welding. These discrepancies persist as a key source of issues. During the welding production process, the material is subjected to temperature distributions that are not uniformly distributed. The repeated heating and cooling cycles produce localized temperature differences, which in turn cause the weld and the surrounding areas to undergo rapid expansions and contractions. Ma et al.'s [2] research result illustrated the thermodynamics and mechanics simulation using the validated finite element model, along with the energy-based damage model, provided insights into the failure mechanisms and damage evolution of the thick steel plate welded joints under complex cyclic loading conditions. Zhang et al.'s [3] study demonstrated the capability of the developed thermo-metallurgical-mechanical coupled model in accurately predicting the residual stress and distortion distribution in the thick steel plate welded joints and provided insights into the underlying mechanisms governing the residual stress

formation. Yang et al. [4] demonstrates the capability of the 2D finite element modeling approach in accurately predicting the temperature field and residual stress distribution in thick steel plate welded joints. It also provides insights into optimizing the welding sequence to effectively mitigate residual stresses.

It has been established that these deformations can cause plastic deformations and residual stresses in the vicinity of the welded structure through their actions. In the long run, these results can impact the fatigue strength of welded structures and damage their quality, performance, and reliability. Additionally, they have the potential to cause difficulties for the entirety of the sessions. Quantifying the fatigue resistance of welded systems has been the subject of a significant amount of study, which includes the utilization of the height stress technique [5]. The potential for welding fractures to spread due to welding has been the subject of additional study [6], which has focused on welding joints' influence on the fitting of layout requirements. Even though welding might generate compressive residual stresses, which may be advantageous in reducing deformations and fracture propagation, it is abundantly clear that this type of information is essential to fulfill the criteria of the product. This involves ensuring the structure is protected and preventing assembly problems and distortions [7]. Many researchers have focused on creating models capable of predicting and contrasting heat distribution, deformations, and residual stresses. In general, it is extremely difficult to properly gather comprehensive records of the distribution of heat, deformations, and residual stresses in welded structures and the use of experimental techniques because these processes are expensive, and there is a possibility that they may result in dimension inaccuracies. To overcome these limitations, it is possible to use the most recent advancements in computational techniques [8, 9].

These strategies simulate welding procedures, quantify residual stresses and distortions, propose welding sequence enhancements, and recognize welding parameters' effects (which include bypass velocity, power, and heat source distribution) on deformation, residual displacement, and pressure fields. These strategies have been proposed. To analyze welded joints, these numerical models usually make use of the Finite Element Method (FEM), with a particular emphasis on transient elastic-plastic thermal-stress evaluations [10]. The simultaneous occurrence of considerable thermal gradients, material non-linearity, temperature-dependent features, and phase transitions is due to extremely complicated numerical models. Consequently, efforts were undertaken to reduce the amount of computing that various numerical approaches need. To do this, it was necessary to provide recommendations on the utilization of temperature-independent material features [11, 12], to carry out parametric studies to lower the expenses of computational work [13], or to suggest clear linkages between material elements and residual stresses [14]. In addition, it is common practice to validate the precision of these complex numerical approaches by contrasting them with actual data [15], even though it may be difficult to get the relevant experimental data. The framework discussed before serves as the foundation for the study described in this article. This paper aims to offer a quantitative and experimental study of the temperature fields formed during the welding process of two low-carbon steel plates to accomplish a butt-welded connection with two passes. Through the utilization of a transient uncoupled thermal-stress finite element method (FEM) analysis, the major purpose of this work was to recreate the welding process. The numerical investigation depended on the new application of the "birth and death" concept suggested by Rubino et al. [16] and Rubino et al. [17]. This complex technique is highlighted in the most recent article by Sepe et al. [18], which highlights its usefulness in modeling welding processes. The paper illustrates the increased applicability of this unique approach.

The objective of this research is to examine how the U joint design impacts the mechanical and thermal characteristics of welds. Additionally, the study aims to develop an engineering simulation model that can be utilized to forecast and compute the mechanical properties of the welding area before the commencement of welding. This is important because rectifying errors after welding has begun can be challenging. This analysis is crucial in the examination of non-standard, yet extensively used, high-thickness plate junction design.

2. EXPERIENTIAL PROCEDURE OF WELDED JOINTS

An experimental sample was fabricated and joined using arc welding techniques to compare the deformation results obtained from the ANSYS model with the actual deformation observed in real conditions and validate the model's results. Two welding joints, a single U joint and an unsymmetrical Double U joint, were designed according to the AWS D1.1 standard, as illustrated in Figure 1(a) and (b), to enhance the realism and validate the accuracy of the simulation model findings.

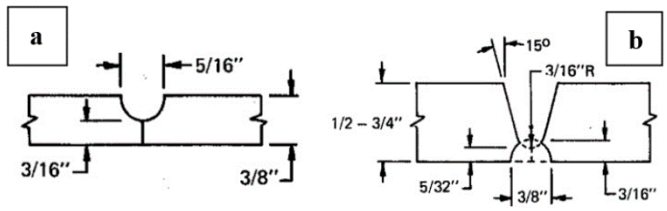

Figure 1. Experimental welding joint sample: (a) single U joint; (b) double U joint

Both joints are supported from the edges to control the deformation. The welding current used in the experimental joint welding is calculated according to the minimum welding temperature required in the welding zone to ensure complete welding electrode and joint melting, which is 1600°C. The welding current can be calculated using the following equations.

$$T_{max.} = (0.4\, q) + T_0 \tag{1}$$

where, T_{max} maximum temperature (°C), q is input welding heat (J/mm), and T_0 base metal temperature (°C). By calculating the value of q the welding current could be calculated from the following equation:

$$q = \frac{UI}{V}\, 0.06 \tag{2}$$

where, q is input welding heat (J/mm), U is arc welding voltage, I is the welding current, and V is welding speed.

3. MODELING OF WELDED JOINTS

The initial stage of welding simulation involves creating a weldment design. High alloy steel welding joints are specifically employed in specialized applications created using SOLIDWORKS software. Two models were made for this investigation: A single U joint without an open root and an Unsymmetrical double U joint as shown in Figure 2. The joint has dimensions of 10 mm in thickness, 50 mm in breadth, and 100 mm in length for each side, as seen in Figure 1(a) and (b). The 3D mechanical models from SOLIDWORKS were loaded into ANSYS to forecast the welding joint temperature profiles, deformation, and residual stresses. The analysis was conducted by starting a thermal analysis of the welding process to forecast heat distribution in the joint design. Thermal analysis results were employed to perform static analysis to predict the stress distribution in welded connections and deformation. Certain assumptions were made throughout the thermal and static investigations. Before welding, the ambient temperature of the basic materials is 22°C. The selection of alloy steel as a simulation material was based on its compatibility with various applications and favorable mechanical and physical qualities. The ANSYS mesh configuration was employed to optimize the distribution and quantity of mesh elements for the welding joint geometry and base metal. The starting thickness of the base metal is set at a constant value of 10 mm.

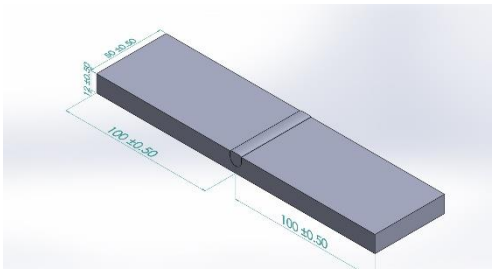

(a)

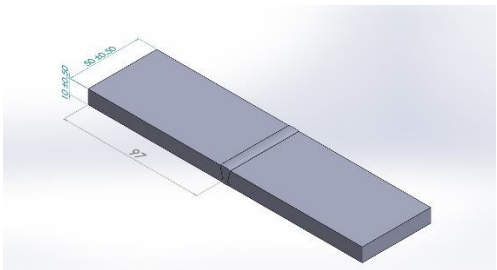

(b)

Figure 2. SOLIDWORKS joint design: (a) U joint; (b) unsymmetrical double U joint

The dimensions of the U joint and unsymmetrical double U joint design mesh elements size were 2 mm for both models. The mesh consisted of 17125 elements and 80718 nodes for a single U joint and 76090 elements and 317005 for a nonequal U joint, with multi-zone mesh mode as seen in Figure 3(a) and (b). The models are fixed at both far edges from the welding joint to simulate the deformation and the stress, the welding heat is applied to the models by selecting the welding joint geometry and applying the welding heat to it as a body. The current study has utilized SOLIDWORKS to simulate the geometric assembly of butt joints and has established its definition based on plate measurements.

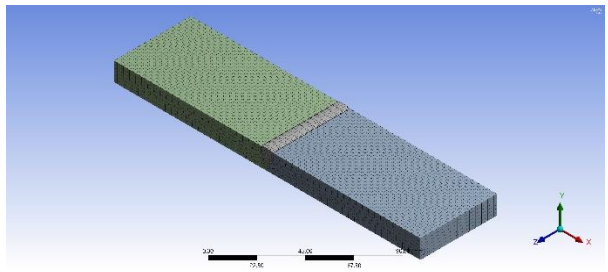

(a)

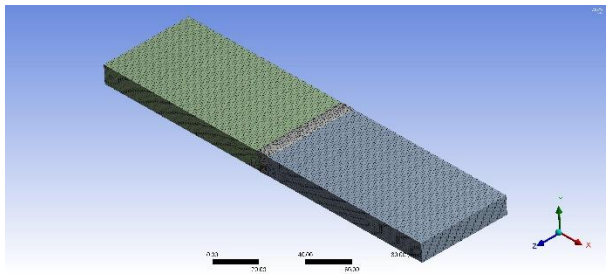

(b)

Figure 3. Joint ANSYS mesh: (a) U joint; (b) unsymmetrical double U joint

4. ANSYS SIMULATION ANALYSIS STEPS

Welding technologies are intricately connected to the fields of mechanics and thermal energy. While the plastic strain that resulted from welding did not substantially impact heat distribution, mechanical and thermal investigation could be carried out independently. Two models must be developed to ensure that the arc welding process is correctly simulated. The initial model must focus primarily on distributing and transporting welding-generated heat. It is recommended that the second model investigate the influence that the distribution of heat has on the mechanical properties and deformation of the part. Calculations of temperature, which are the foundation of both models, would affect the entire welding process. A significant component that plays a role in these calculations is the thermophysical and mechanical properties of the base metal. This experiment made use of alloy steel plates, and Table 1 contains a listing of the material parameters of those plates. Specific heat, thermal conductivity, yield stress, thermal expansion coefficient, and Poisson's ratio as a function of temperature are some of the features included in this discussion.

Table 1. Alloy steel plates' physical and mechanical properties

Elastic modules	200 GPa
Poisson rate	0.33
Shear modules	80 GPa
Mass density	7850 kg/m^3
Tensile strength	460 MPa
Yield strength	250 MPa
Thermal expansion	1.2×10^{-5} mm/°C

5. ANSYS MODEL THERMAL ANALYSIS EQUATIONS

One of the most important concepts to consider when examining heat flow in welding is energy conservation. This

concept can solve a solid structure's fundamental equation for heat conduction. As shown in Figure 3, an appropriate mesh optimization method from ANSYS is utilized to generate a relatively thin mesh for the base metal and welding joints of both U and double U joints that have been selected for thermal analysis. The thermal field is governed by the equation that determines the Fourier law of heat conduction, which is supplied by:

$$q = -KA\left(\frac{dt}{dX}\right) \tag{3}$$

To compute the heat transfer rate, or q, which is stated in watts, the material's thermal conductivity, denoted by the symbol k and measured in watts per meter by ℃, is utilized. The cross-sectional area (A), measured in square meters, is the region throughout which heat is transmitted. Variation in temperature by unit distance within the direction of heat flow is referred to as the temperature gradient, and it is stated in ℃ per meter and written as (dt/dx). According to the equation, the rate of heat transfer (q), the cross-sectional location (A), and the temperature gradient (dt/dx) are all connected at the same time to the same degree. From one region with a higher temperature to another region with a lower temperature, it depicts the passage of heat through a material from one region to another. The heat flow density for convection (q_c) is calculated by Newton's equation of heat transfer in an environment that is either a gas or a liquid atmosphere:

$$q_c = \rho(T)h_c(T - T_0) \tag{4}$$

The convective heat transfer coefficient is denoted by h_c, T_0 denotes the temperature of the gas or liquid, and the temperature of the surface exposed to the environment is denoted by T. Environment, surface properties, and the circumstances of convection on a solid surface all have a role in determining this coefficient. It has been hypothesized by authors such as Gery et al. [19] that the values for the convective heat transfer coefficient would fall somewhere between 15 and 25 W/m^{2}K. The radial position r, which originates at the center of the arc, is said to be connected to the distribution of heat flux on a solid surface. Welding problems may be caused by three types of heat flux: Convective heat, irradiative heat, and boundary heat. If we want to explain the heat flux losses that occur on welded plate surfaces due to convection and radiation, respectively, we may use Eqs. (5) and (6):

$$q_c = h(T - T_o) \tag{5}$$

$$q_e = \varepsilon\, \xi\, (T^4 - T_0^4) \tag{6}$$

where, T_0 is the room temperature, ξ is Stefan Boltzmann constant, and h, $\acute{\varepsilon}$ are convection and emissivity coefficients for all plate surfaces. In this study, flux losses due to the radiation are not considered. In addition, the latent heat of fusion is supposed to feel the phase transformation.

6. MECHANICAL ANALYSIS EQUATIONS

The mathematical models and numerical analysis of welding joints are the most effective methods for predicting welding heat distribution and thermal, elastic, plastic, and residual stress models. The microstructure, volume, and phase transformation changes that occur at welding joints, as well as the heat-affected zone (HAZ), may be predicted using welding heat distribution models. This is because phase transformation occurs at a very low temperature (723 degrees Celsius). The subsequent mechanical qualities may be predicted with this help. In welding thermal analysis, the distribution of temperatures is analyzed and recorded for every joint design. After some time, this information is utilized in the mechanical analysis as thermal loading to construct the thermal stress field. This opens the way for calculating thermal strain and stress over the whole design. From the perspective of the isotropic strain hardening rule and the Von Mises yield criteria, the stress-strain relations in the thermal elastoplastic material model may be described as follows:

$$\varepsilon_{total} = \varepsilon_e + \varepsilon_p + \varepsilon_t \tag{7}$$

Here is an expression for the constitutive equation that should help us grasp it:

$$\sigma = D = D(\varepsilon_{total} - \varepsilon_p - \varepsilon_t) \tag{8}$$

The material stiffness matrix, denoted by the letter D, was the foundation for the model that modeled elastic-plastic behavior with linear kinematic hardening. Upon reaching the melting point, the yield stress of most alloy steels completely disappears after a precipitous decrease that occurs as the temperature rises. The thermal stresses, strain, and deformation caused by a thermal load were estimated using ANSYS. This load was created by applying the alloy steel melting temperature of 1600℃ to the welding zone of the joints that were being tested. The weldment's left and right sides were set to simulate the conditions encountered in real life.

7. NUMERICAL MODEL AND FINITE ELEMENT ANSYS SIMULATION CALCULATIONS

The investigation of joint designs for fusion welding is a two-step procedure that is analogous to the process of resolving a separate problem. The design of the welding joint served as the basis for a thermal study that was performed to predict the distribution of welding temperatures during the welding process. Following that, the authors conducted a mechanical engineering analysis to ascertain the welding thermal loads. This inquiry determined and evaluated the distribution of residual stress and deformation. A diagrammatic representation of the flow of this analytical method is shown in Figure 4. A fundamental presumption underpinning this simulation was that variations in temperature and mechanical states would be responsible for controlling mechanical characteristics.

Both sides of the weldment have geometric dimensions of 200×50×10 mm, and the simulation is carried out with the assistance of the ANSYS program. At a temperature of 1600℃, the weld metal is heated, and the mechanical and chemical properties of the welding material are equivalent to those of actual tank welding work [20]. At the beginning, the temperature of the parent material is 22℃. In welding, some parameters utilized include the distribution of heat input, thermal gradients, the fusion zone (FZ) border, and the heat-affected zone (HAZ).

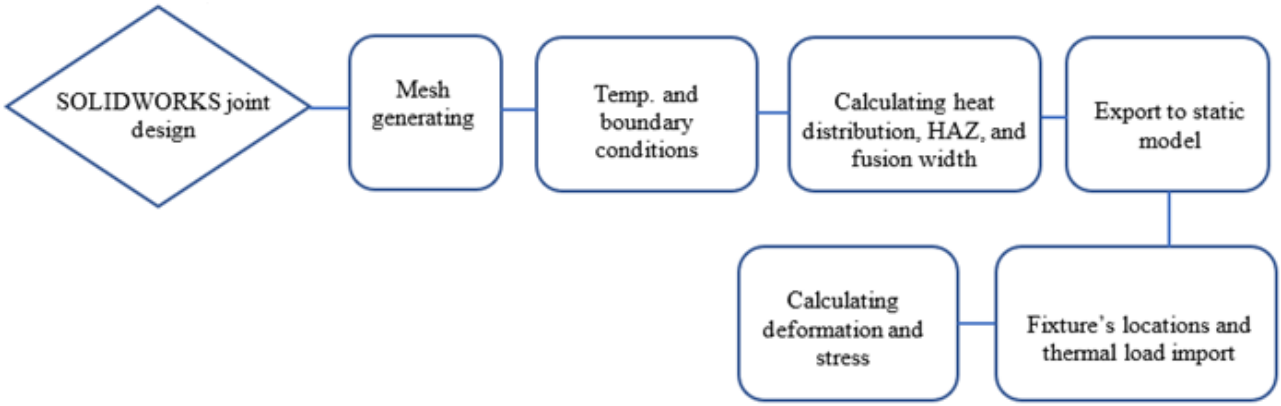

Figure 4. Thermal and mechanical analysis flow chart

According to the AWS D1.1 standard, the welding current used in this experiment was 400A, and the voltage was 35 volts. The welding travel speed in Eq. (2) is calculated using the lowest critical welding cooling rate of alloy steel, which is the rate at which martensite does not occur in the microstructure of the welding zone. According to the T.T.T diagram for allot steel, a cooling rate of 140°C per second is required. It is possible to utilize the thick plate critical cooling rate (C.C.R.) and the welding heat input (H net) as given in Eq. (7) to determine the welding travel speed (V) that did not result in the production of martensite. And at a rate of 1.38 millimeters per second. For the welding process, a heat input of 606.7 will be necessary.

$$C.C.R. = 2\pi K(Tc - To)^2 / H_{net} \quad (9)$$

where, *C.C.R.* is the critical cooling rate, *K* is thermal conductivity, *Tc* is the critical temperature 550°C, the initial temperature is 30°C, and H_{net} welding heat input is 606.7.

8. RESULTS AND DISCUSSION

8.1 Heat distribution model

The estimated temperature fields and HAZ size from the fusion line and the weld penetration were verified by ANSYS by measuring the temperature distribution for the two models in different locations. To model the distribution of welding heat in ANSYS, we use SOLIDWORK models of welding joints equipped with welding beads; we apply welding heat to these models by selecting the section of the joint. This distribution is critical for determining the distance between the welding fusion line and the (723°C) edge, where the phase transformation would occur; no phase transformation occurs below this temperature. Figure 5 and Figure 6 show the ANSYS calculation of the HAZ width from the welding fusion line for the two joints design. Based on the ANSYS model, the findings show that the joint HAZ width was 45.4 mm from the fusion line, with the fusion zone measuring about 1.2 mm for a single U joint and 53.6 mm HAZ width with a 2.7 mm fusion zone for a double U joint. Figure 5(a) shows the full joint penetration of a single U joint with this thickness.

The phase transformation rules served as the foundation for the metallurgical analysis conducted in this work [19]. Heat distribution models were utilized to predict the phase shift during welding. According to the regulations, the pearlite-ferrite in the base metal may partially transform into austenite if the temperature of the pearlite-ferrite is raised to a level higher than the cementite disappearance temperature (A_1). When the temperature is raised to a higher level than the a-ferrite disappearance temperature (A_3), the material transforms into austenite. Estimating the welding heat distribution and the HAZ width is essential to appreciate this shift and foresee the subsequent microstructure. Calculating the temperatures of low alloy steel A_1 and A_3 requires applying the equations presented in the study of Teng et al. [20].

$$A_1 = 723 - 10.7\,\text{Mn} - 16.9\,\text{Ni} + 29\,\text{Si} + 16.9\text{Cr} + 290\,\text{As} + 6.4\,\text{W} \quad (10)$$

$$A_3 = 912 - 203\sqrt{c} - 15.2\,Ni + 44.7\,Si + 104\,V + 31.5\,Mo + 13.1\,W - 30\,Mn - 11\,Cr - 20\,Cu + 700\,P + 400\,Al + 120\,As + 400\,Ti \quad (11)$$

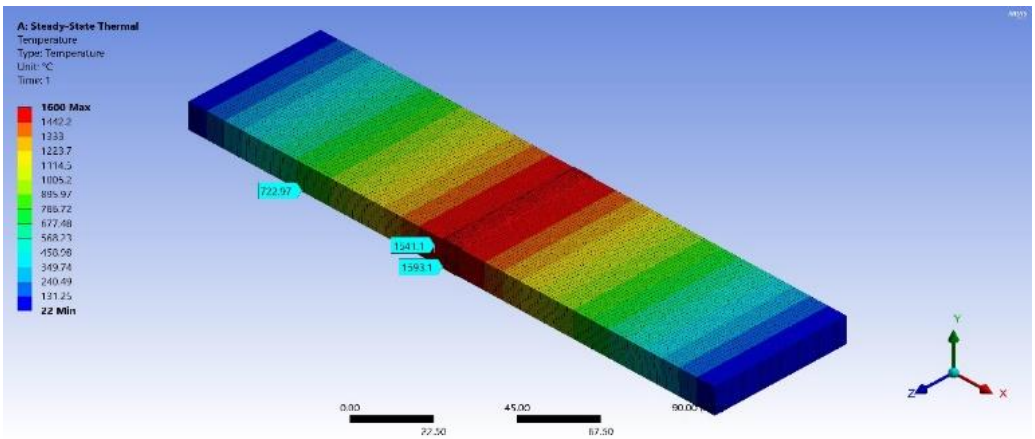

(a)

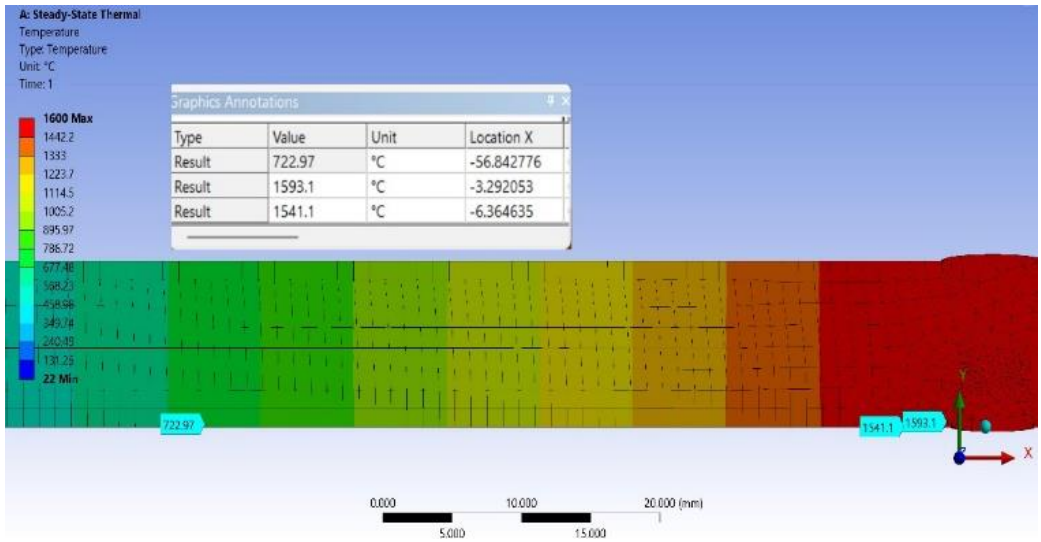

(b)

Figure 5. U joint ANSYS model heat distribution: (a) U joint heat distribution; (b) HAZ, and fusion zone width from the welding fusion

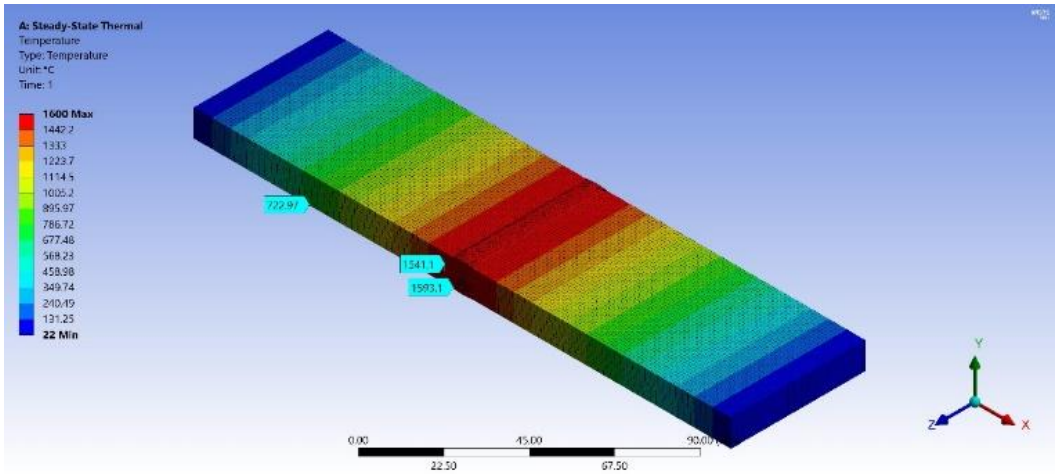

(a)

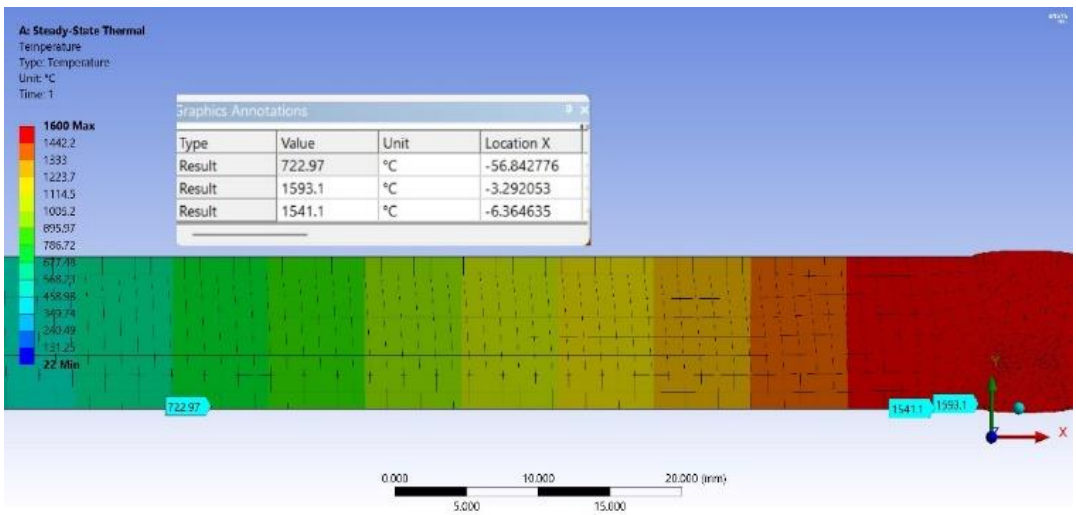

(b)

Figure 6. Double U joint ANSYS model heat distribution: (a) Double U joint heat distribution; (b) HAZ, and fusion zone width from the welding fusion

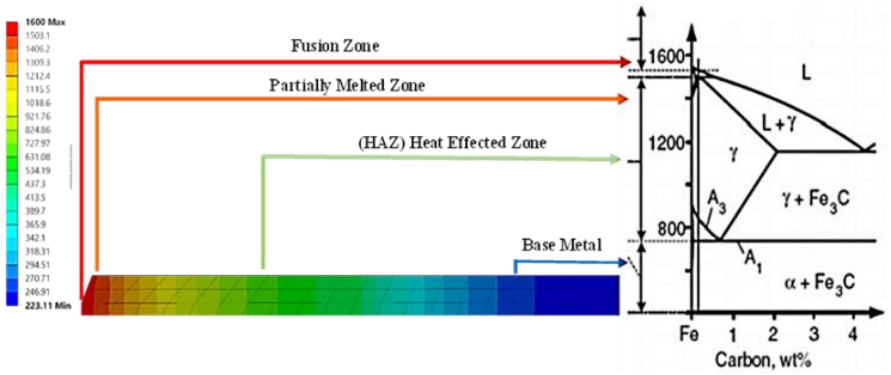

Figure 7. Alloy steel phase transformations map

After using the previous formulas, the estimated temperatures of A_1 and A_3 will be 723 and 912°C, respectively. When the temperature of the heat-affected zone (HAZ) climbs above the temperature of the A1 zone, the body-centered cubic structure (BCC) transforms into a face-centered cubic structure (FCC), reducing its volume. Figure 7 provides a schematic illustration of the thermal map zones defined by the welding heating in the welding zone and the HAZ.

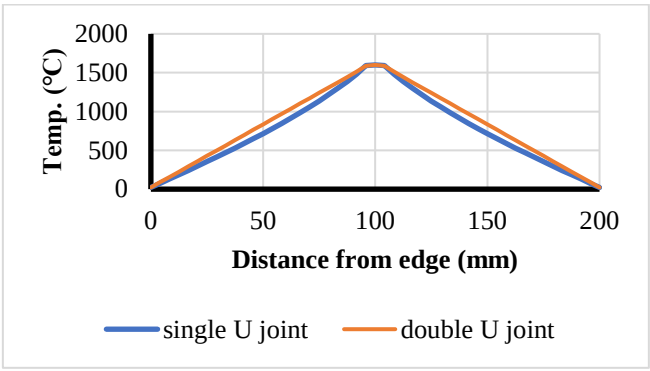

Figure 8. Welding U joint and unsymmetrical double V joint heat distribution along the X-axis weldment

The authors created a distance-temperature gradient map connecting the molten zone of the welding center and the weldment edge with the help of the ANSYS thermal distribution data along the X-axis of the weldment; this made it possible to receive an exact thermal estimate. A visual representation of the joint's heat dispersion may be seen on the graphs. Microstructure, mechanical characteristics, and the required distance from the center line were all displayed in Figure 8. Both models' temperature gradient data show almost the same heat distribution diagram. However, a fast cooling rate can be noticed with a single U joint temperature gradient diagram, decreasing the HAZ width. Also, as shown in Figure 1(a), the U joint design results in more welding heat absorption by the solid metal below the U groove to reach the melting point, increasing the molten filler cooling rate and reducing both the HAZ and FZ width. By utilizing this model to forecast the temperatures of experimental joints for applications in the real world, welding engineers and specialists would save a significant amount of time. It is essential to have a solid understanding of the depth to which the molten metal will penetrate when planning welding connections and when calculating the welding zone and the mechanical characteristics of the weld once it has been created. In addition to being directly proportional to the volume of molten material, this depth is also directly related to the amount of heat introduced into the welding process, which increases as the welding current increases. Because the volume increases with each advancement in penetration depth, reinforcement height, and weld width [21], the impacted surface area receives the heat. This results in the penetration depth increasing to compensate for the increased volume.

7.1 ANSYS model deformation and stress

The thermal stresses in the welded joints of the structure are similar to those seen in laboratory-designed model plates. The joint's shape and the material properties of the parts being welded are crucial considerations when choosing the welding procedure. The tensions in the plastic deformation zone may change as a result of structural alterations occurring in the metals being welded [22]. Welding in this manner allows for complete gap coverage and structural integrity, but it also increases the level of residual stress in the heat-affected zone of the welded joint simultaneously. This limitation on the weldment edges would result in the transmission of all deformation and stress toward the side of the joint that is not connected. The experimental models were secured at the two weldment edges using ANSYS software to calculate thermal deformation and thermal stress. This was conducted to replicate the environmental conditions seen during storage tank welding procedures. The movement of dislocations and the migration of atoms are closely linked, and both processes play a crucial role in the deformation of materials. Plasticity refers to the situation where dislocation motion is the primary mechanism.

Deformation, or diffusional flow, refers to the phenomenon when atom diffusion is the dominant process. The phrase "plastic deformation" can also encompass phase changes, but transformation strains typically encompass phase shifts. The model proposed by Yadegari and Turteltaub in their research paper [23] was based on dislocation density. The model explains one of the elements that contribute to the overall inelastic strain rate. Moreover, it illustrates how various techniques collectively contribute to the flow stress. The model proposes that the flow stress is composed of contributions from obstacles that interact with dislocations in motion. Because the former is athermal [24], thermal energy cannot aid dislocations in surmounting the deformed portions of the lattice [24]. Thermally induced processes can help dislocations overcome obstacles that are nearby. The dislocation and tension hindered the restoration of the welding edges to their original state in both the welding and heat-affected zones (HAZ). The occurrence of the maximum deformation in the welding zone and later in the heat-affected zone (HAZ) was a result of the high thermal load and

temperature gradient in these areas during welding. Figure 9(a) depict the ANSYS analysis findings of the thermal deformation of both the single U and double U joint ANSYS models, as shown in a graphical diagram. The diagram exhibited nearly identical distortion for both models. However, the decrease in deformation value in the Heat Affected Zone (HAZ) will be more significant when using a single U joint because of the intense heat dissipation, as illustrated in Figure 8. Figures 10(b) and (c) illustrate the precise location where the maximum deformation calculation is performed. The chart illustrates significant deformation at the welding joint's upper front face centre along the x-axis, which is attributed to the elevated heat input during welding. The single U joint exhibited a maximum deformation value of 0.553 mm, while the double U joint showed a maximum deformation value of 0.547 mm. The deformation in the direction of the weldment edges decreased due to the dispersion of heat and the presence of two edges, which hindered the development of thermal stress in the structure. This is illustrated in Figure 9(a-c). Additionally, no residual stress occurred as a result of the transformation of phases behind the heat-affected zone (HAZ) dimension. This had a significant impact on the mechanical properties of the weldment and the progression of deformation. The deformation was nearly equal for both models, despite the double U joint having a greater volume of welding metal, indicating more input heat and deformation. However, this joint design necessitated welding from both sides. As a result, the high deformation on the upper side, caused by a large amount of filler metal and high heat input, was reduced when welding the lower joint side from the opposite direction. This led to a reduction in deformation on the upper side caused by welding. The points of maximal distortion for both joints will occur at the starting and ending sections of the welding joint, as depicted in Figure 9(b) and (c).

Thermal stresses generated during welding primarily cause dislocations and phase changes in the welding and heat-affected zones (HAZ). This is a widely recognized truth. By employing a decompositional strategy that permits the separation of their rates in an additive way, it becomes feasible to attribute all stresses in welding structures to the elastic strains (ɛe) using the fundamental principles of the thermal stress law. These strains rely heavily on the other components of these strains to function well. The primary causes of these stresses are the inherent asymmetry of the interatomic potential and the temperature changes that rely on the composition of the lattice. With a temperature rise, it is inevitable for a strain to increase due to the expansion of the average interatomic distance. Furthermore, transition strains refer to additional instances of straining that might arise from separate alterations in the crystal structure. The stresses induce distinct modifications in the microstructure. To minimize deformation in the welding joint, it is necessary to reduce the thermal stresses caused by the input heat from welding or provide a means for them to dissipate. The welding heat often causes this region to be structurally inferior to the base metal, even when the temperature is unchanged. The thermal strain will propagate in the same direction as the heat flow, moving from the high-temperature melting zone of the welding joint towards the heat-affected zone (HAZ) and then to the base metal. The primary reason for the occurrence of welding deformation is the base metal margins, which are situated at a considerable distance from the welding joint. However, in real welding scenarios where the edges of the weldment are securely fastened and the weldment itself is thick, indicating a significant amount of heat input and molten metal deposition, the strain value would be exceptionally high in this simulation. The molten metal would return to the welding joint and collect within it, causing a substantial increase in thermal stress that exceeds the strength of the base metal.

Simultaneously, the liquefied mixture of filler metal and base metal employed in welding can adjust to this heightened stress, diminish it before solidification, and convey it to the high-risk area known as the heat-affected zone (HAZ). Nevertheless, despite that, the thermal stress value remains significantly elevated, beyond the threshold required to induce a discernible deformation of around 0.5% of the weldment's thickness, specifically within the welding joint. Figure 10 demonstrates that the stress level significantly decreased after the fusion zone and became almost negligible after 5 mm from the welding zone. The ANSYS software was used in this study to numerically estimate the critical distance at which this stress occurs in joint design. This distance begins when the stress exceeds the 240 Mpa range, which is the yield strength of the alloy steel. Beyond this range, towards the fusion zone, the weldment will experience permanent deformation. Based on the information provided in Figure 10, the thermal stress range for both U joint designs will be approximately 5 millimeters from the welding centre and at the boundaries. However, the welding joint centre will exhibit the highest level of distortion, while the two edges will remain unaffected due to the fixings. The zone referred to is the primary origin of the greatest amount of thermal energy input, resulting in the most significant levels of stress and deformation within the welded joint. The results demonstrate the correlation between the overall volume of filler placed into the joints and the critical range of thermal stresses. The findings indicate that the thermal impacted range expanded proportionally with the increase in the amount of deposited metal. The overall heat input to the welding area has increased, resulting in a significant temperature difference between the joints.

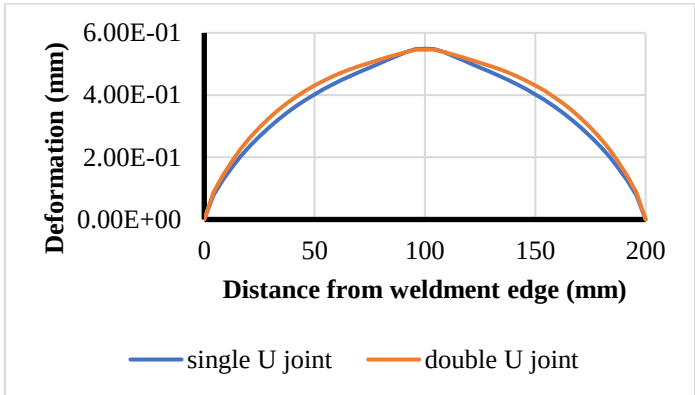

(a)

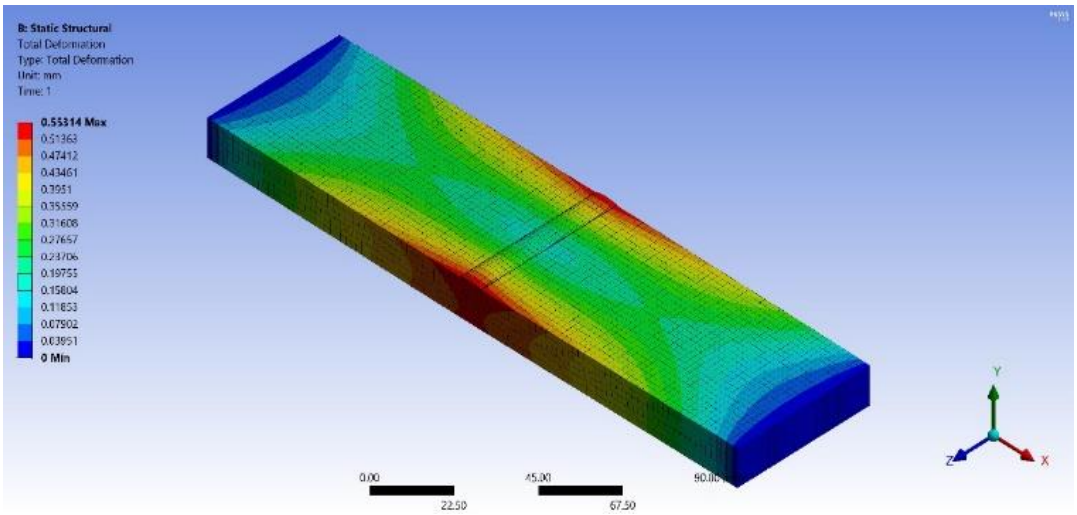

(b)

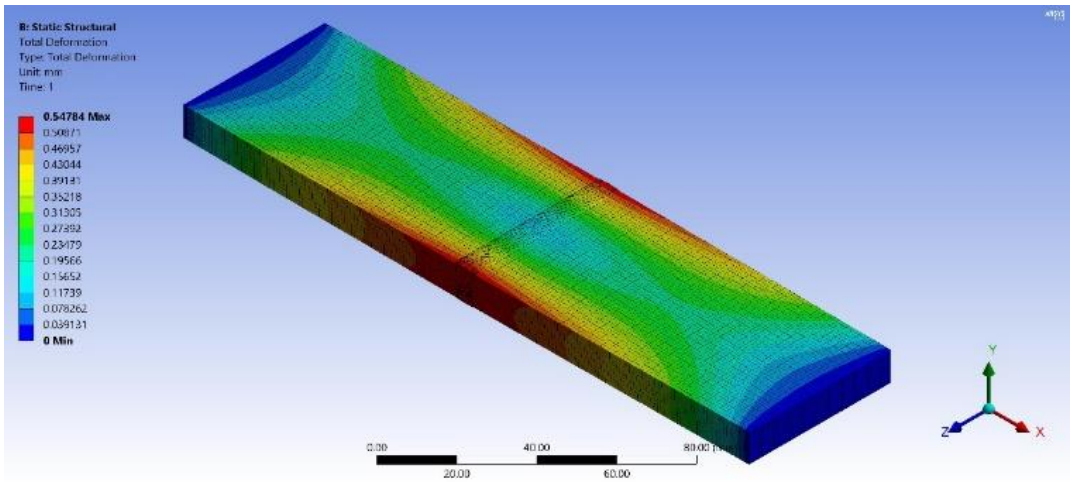

(c)

Figure 9. (a) Single U and unsymmetrical double u joint deformation diagram; (b) U joint deformation; (c) Unsymmetrical double V joint deformation

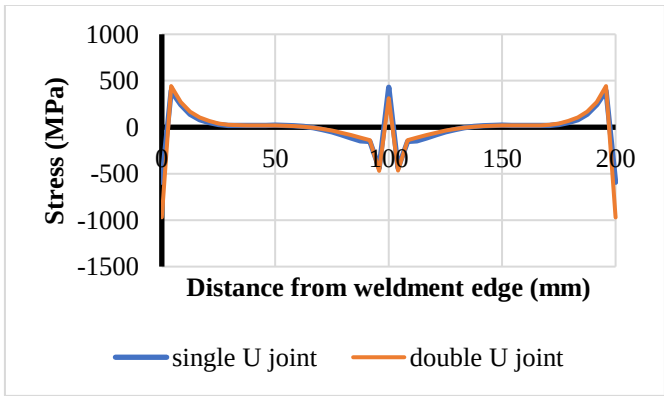

(a)

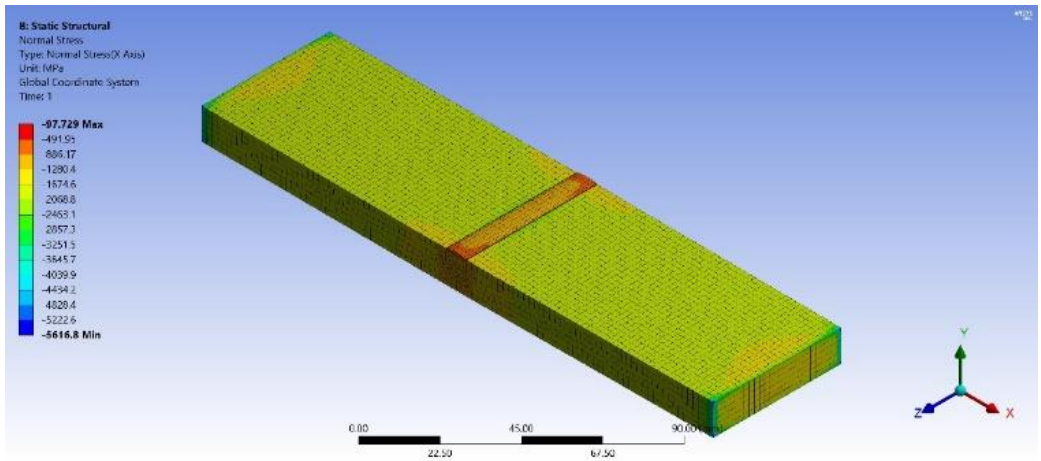

Figure 10. (a) single U joint and unsymmetrical double U joint stress diagram; (b) single U joint stress; (c) unsymmetrical double U joint stress

The liquid amalgamation of filler and base metals possesses the ability to adapt to increasing strain, diminish it before to solidification, and convey it to the heat-affected zone (HAZ) during the welding process. However, the thermal stress value remains very high, indicating that it is more than sufficient to create noticeable deformation within the welding joint, which can vary from 0.5% of the weldment's thickness. The ANSYS software was used to calculate the critical distance of stress in joint design by numerical estimation. Once the stress level reaches the 240 Mpa threshold, the measurement of the yield strength and distance of the alloy steel commences from that point onwards. Figure 10(a) demonstrates that both the U joint and double U joint weldments will experience permanent deformation beyond this range. The reason for this is that the stress in the welded structure decreased significantly after the fusion area and became nearly negligible after a distance of 5 mm from the welding zone. Both joint designs will incorporate a thermal stress critical range of 5 millimeters, as depicted in Figure 10. This range will be located at both the welding center and the margins. In contrast, the fixings will not cause any deformation on either side, while the center of the welding joint will result in the highest level of distortion. The welding joint experiences the maximum level of stress and deformation in this specific region, primarily because it receives the most intense heating input. These findings establish a correlation between the extent of significant heat pressures and the total amount of filler material accumulated within the joints. Based on the data depicted in Figures 10(b) and (c), it can be observed that the higher quantity of filler metal applied to the upper side of the welding joint led to a greater level of stress compared to the lower side, which had a lower amount of filler. This was the situation with the asymmetrical dual universal joint. The thermal affected range expanded as the amount of metal deposited grew due to the wide temperature gradient range resulting from the increase in total input heat to the welding zone. This is likely due to the wide variety of temperature gradients that were generated. The disparity between the two schematics of both joints is seen in the peak stress observed at the two attachment locations. The double U joint experiences a maximum stress value of 970.38 MPa at these places, while the single U joint has a maximum stress value of 592.43 MPa. These data demonstrate the impact of increasing the volume of molten filler metal deposited on the tension of the welding joint.

Figure 9 displays the computed welding deformations. These deformations are used to compare the results obtained from the simulation with those obtained from the real welding operation. Table 2 illustrates the distinctions between the two approaches.

Several factors might cause the simulation results to differ somewhat from the welding process. These include the location of the fixture, the welding cooling rate, and the welding speed. These elements directly influence the amount of heat input, and they are accountable for producing the results.

Table 2. Actual welding and ANSYS simulation deflection results comparison

Joint Design Type	Max. Deformation (mm)	
	ANSYS	Welding
Single U joint	0.55	0.43
Unsymmetrical double U joint	0.54	0.46

9. CONCLUSIONS

The current investigation used the numerical simulation software ANSYS and SOLIDWORKS programs to carry out mechanical and thermal stress simulations within the butt weld of thick alloy steel plates. During the research, two U-joint joints were created and examined, and the following findings were discovered:

1. Regarding the distribution of weld heat, the HAZ width was approximately 45.4 mm from the fusion line, with the fusion zone measuring about 1.2 mm for a single U joint and 53.6 mm HAZ width with a 2.7 mm fusion zone for a double U joint. Also, the results illustrated a full joint penetration for the single U joint.
2. According to the ANSYS simulation, the highest distortion in a single U joint was determined in the center of the weldment face side, both at the beginning and end of the welding joint line. The unsymmetrical double U joint exhibited a deformation of 0.54 mm at both locations. However, the magnitude decreased as one moved towards the periphery of the weldments, owing to the specific circumstances prevailing in those areas.
3. The thermal stress results revealed that the highest stress occurred in the weld metal for both joints and rapid drop in the HAZ. The critical range of thermal stress that can lead to irreversible distortion has been identified to investigate both joint design in the center of welding joints and the two weldments' edges and become non-affected after 5 mm from the welding joint center line.
4. The link between the critical range of thermal stresses and the total volume of filler in joints is shown by the maximum unsymmetrical double U joint weldment stress value at the two fixed edges. Stress was greater on the top side of the asymmetrical double U welding joint due to the higher metal filler quantities than on the bottom side, which had lower filler amounts. The temperature gradient range caused by increased total input heat to the welding zone probably explains why the thermal impacted range grew in tandem with the metal deposition rate.
5. The residual stresses, thermal effects, and plastic deformations make finite element simulations valuable for studying welding processes. These simulations are necessary because they provide essential knowledge that can be used to improve the joint design and the welding parameters to minimize any negative impact of welding on the mechanical properties of the weldment. Then, they evaluate the simulation data with experimental tests and refine modern welding methods that reduce thermal stresses and distortion.

REFERENCES

[1] Astarita, A., Tucci, F., Silvestri, A.T., Perrella, M., Boccarusso, L., Carlone, P. (2021). Dissimilar friction stirs lap welding of AA2198 and AA7075 sheets: Forces, microstructure, and mechanical properties. International Journal of Advanced Manufacturing Technology, 117: 1045-1059. https://doi.org/10.1007/s00170-021-07816-7

[2] Ma, H.W., Zheng, H., Zhang, W., Tang, Z.Z., Lui, E.M. (2020). Experimental and numerical study of mechanical behavior of welded steel plate joints. Metals, 10(10): 1293. https://doi.org/10.3390/met10101293

[3] Zhang, K.Y., Dong, W.C., Lu, S.P. (2022). Residual stress and distortion in thick-plate weld joint of AF1410 steel: Finite element simulations and experimental studies. Materials Research Express, 9(1): 016524. https://doi.org/10.1088/2053-1591/ac4c5d

[4] Yang, X.Y., Yan, G.Z., Xiu, Y.F., Yang, Z.W., Wang, G., Liu, W., Li, S.H., Jiang, W.C. (2019). Welding temperature distribution and residual stresses in thick welded plates of SA738Gr.B through experimental measurements and finite element analysis. Materials, 12(15): 2436. https://doi.org/10.3390/ma12152436

[5] Barsoum, Z., Barsoum, I. (2009). Residual stress effects on fatigue life of welded structures using LEFM. Engineering Failure Analysis, 16(1): 449-467. https://doi.org/10.1016/j.engfailanal.2008.06.017

[6] Abtan, A.A., Mohammed, M.S., Alshalal, I. (2024). Microstructure, mechanical properties, and heat distribution ANSYS model of CP copper and 316 stainless steel torch brazing. Advances in Science and Technology Research Journal, 18(1): 167-183. https://doi.org/10.12913/22998624/177299

[7] Citarella, R., Carlone, P., Lepore, M., Sepe, R. (2016). Hybrid technique to assess the fatigue performance of multiple cracked FSW joints. Engineering Fracture Mechanics, 162: 38-50. https://doi.org/10.1016/j.engfracmech.2016.05.005

[8] Dauod, D.S., Mohammed, M.S., Aziz, I.A.A., Abbas, A.S. (2023). Mechanical vibration influence in microstructural alterations and mechanical properties of 304 stainless steel weld joints. Journal of Engineering Science and Technology, 18(6): 33-54. https://www.researchgate.net/publication/377724682.

[9] Perić, M., Garašić, I., Tonković, Z., Vuherer, T., Nižetić, S., Dedić-Jandrek, H. (2019). Numerical prediction and experimental validation of temperature and residual stress distributions in buried-arc welded thick plates. International Journal of Energy Research, 43(8): 3590-3600. https://doi.org/10.1002/er.4506

[10] Murugan, S., Kumar, P.V., Raj, B., Bose, M.S.C. (1998). Temperature distribution during multipass welding of plates. International Journal of Pressure Vessels and Piping, 75(12): 891-905. https://doi.org/10.1016/S0308-0161(98)00094-5

[11] Bhatti, A.A., Barsoum, Z., Murakawa, H., Barsoum, I. (2015). Influence of thermo-mechanical material properties of different steel grades on welding residual stresses and angular distortion. Mater & Design, 65: 878-889. https://doi.org/10.1016/j.matdes.2014.10.019

[12] Sepe, R., Greco, A., De Luca, A., Caputo, F., Berto, F. (2021). Influence of thermo-mechanical material properties on the structural response of a welded butt-joint by FEM simulation and experimental tests. Forces in Mechanics, 4: 100018. https://doi.org/10.1016/j.finmec.2021.100018

[13] Sepe, R., Armentani, E., Lamanna, G., Caputo, F. (2015).

Evaluation by FEM of the influence of the preheating and post-heating treatments on residual stresses in welding. Key Engineering Materials, 627: 93-96. https://doi.org/10.4028/www.scientific.net/KEM.627.93
[14] Armentani, E., Esposito, R., Sepe, R. (2007). The influence of thermal properties and preheating on residual stresses in welding. International Journal of Computational Materials Science and Surface Engineering, 1(2): 146-162. https://doi.org/10.1504/IJCMSSE.2007.014870
[15] Armentani, E., Pozzi, E., Sepe, R. (2014). Finite element simulation of temperature fields and residual stresses in butt welded joints and comparison with experimental measurements. In Proceedings of the ASME 2014 12th Biennial Conference on Engineering Systems Design and Analysis, Copenhagen, Denmark. https://doi.org/10.1115/ESDA2014-20541
[16] Rubino, F., Parmar, H., Esperto, V., Carlone, P., (2020). Ultrasonic welding of magnesium alloys: A review. Materials and Manufacturing Processes, 35(10): 1051-1068. https://doi.org/10.1080/10426914.2020.1758330
[17] Rubino, F., Esperto, V., Paulo, R.M.F., Tucci, F., Carlone, P. (2020). Integrated manufacturing of AA6082 by friction stir welding and incremental forming: Strain analysis of deformed samples. Procedia Manufacturing, 47: 440-444. https://doi.org/10.1016/j.promfg.2020.04.331
[18] Sepe, R., Giannella, V., Greco, A., De Luca, A. (2021). FEM simulation and experimental tests on the SMAW welding of a dissimilar T-joint. Metals, 11(7): 1016. https://doi.org/10.3390/met11071016
[19] Gery, D., Long, H., Maropoulos, P. (2005). Effects of welding speed, energy input and heat source distribution on temperature variations in butt joint welding. Journal of Materials Processing Technology, 167(2-3): 393-401. http://doi.org/10.1016/j.jmatprotec.2005.06.018
[20] Teng, T.L., Chang, P.H., Tseng, W.C. (2003). Effect of welding sequences on residual stresses. Computers & Structures, 81(5): 273-286. https://doi.org/10.1016/S0045-7949(02)00447-9
[21] Dossett, J.L., Totten, G.E. (2013). Steel heat treating fundamentals and processes. ASM Handbook. https://doi.org/10.31399/asm.hb.v04a.9781627081658
[22] Nigay, R., Nigay, E., Mironova, L. (2020). Investigation of thermal and deformation processes in the welding of shell structures made of carbon and high-alloy structural steels. Journal of Physics: Conference Series, 1431: 012039. https://doi.org/10.1088/1742-6596/1431/1/012039
[23] Yadegari, S., Turteltaub, S., Suiker, A.S.J. (2012). Coupled thermomechanical analysis of transformation induced plasticity in multiphase steels. Mechanics of Materials, 53: 1-14. doi.org/10.1016/j.mechmat.2012.05.002
[24] Lindgren, L.E., Domkin, K., Hansson, S. (2008). Dislocations, vacancies and solute diffusion in physical based plasticity model for AISI 316L. Mechanics of Materials, 40(11): 907-919. https://doi.org/10.1016/j.mechmat.2008.05.005